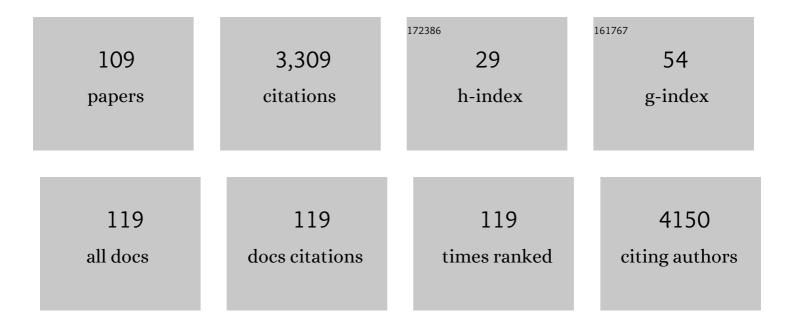
Graham J Galloway

List of Publications by Year in descending order

Source: https://exaly.com/author-pdf/2780315/publications.pdf Version: 2024-02-01



#	Article	IF	CITATIONS
1	Case Report: Capacity to Objectively Monitor the Response of a Chronic Pain Patient to Treatment. , 2022, 1, .		0
2	A global view of standards for open image data formats and repositories. Nature Methods, 2021, 18, 1440-1446.	9.0	36
3	A Preclinical Animal Model for the Study of Scaffold-Guided Breast Tissue Engineering. Tissue Engineering - Part C: Methods, 2021, 27, 366-377.	1.1	6
4	Increased GABA+ in People With Migraine, Headache, and Pain Conditions- A Potential Marker of Pain. Journal of Pain, 2021, 22, 1631-1645.	0.7	14
5	7-Tesla Functional Cardiovascular MR Using Vectorcardiographic Triggering—Overcoming the Magnetohydrodynamic Effect. Tomography, 2021, 7, 323-332.	0.8	3
6	Increase in ACC GABA+ levels correlate with decrease in migraine frequency, intensity and disability over time. Journal of Headache and Pain, 2021, 22, 150.	2.5	9
7	Magnetic Resonance Imaging and Micro-Computed Tomography reveal brain morphological abnormalities in a mouse model of early moderate prenatal ethanol exposure. Neurotoxicology and Teratology, 2020, 77, 106849.	1.2	3
8	GABAa receptor density alterations revealed in a mouse model of early moderate prenatal ethanol exposure using [18F]AH114726. Nuclear Medicine and Biology, 2020, 88-89, 44-51.	0.3	2
9	Hexarelin targets neuroinflammatory pathways to preserve cardiac morphology and function in a mouse model of myocardial ischemia-reperfusion. Biomedicine and Pharmacotherapy, 2020, 127, 110165.	2.5	6
10	Early gestational ethanol exposure in mice: Effects on brain structure, energy metabolism and adiposity in adult offspring. Alcohol, 2019, 75, 1-10.	0.8	10
11	Post-traumatic stress disorder affects fucose-α(1–2)-glycans in the human brain: preliminary findings of neuro deregulation using in vivo two-dimensional neuro MR spectroscopy. Translational Psychiatry, 2019, 9, 27.	2.4	5
12	Two New Fucose-α (1–2)-Glycans Assigned In The Healthy Human Brain Taking The Number To Seven. Scientific Reports, 2019, 9, 18806.	1.6	9
13	Putting the Trust into Trusted Data Repositories: A Federated Solution for the Australian National Imaging Facility. International Journal of Digital Curation, 2019, 14, 102-113.	0.1	2
14	Hexarelin treatment preserves myocardial function and reduces cardiac fibrosis in a mouse model of acute myocardial infarction. Physiological Reports, 2018, 6, e13699.	0.7	12
15	Intramuscular fat is present in cervical multifidus but not soleus in patients with chronic whiplash associated disorders. PLoS ONE, 2018, 13, e0197438.	1.1	14
16	Altered functional connectivity in mesial temporal lobe epilepsy. Epilepsy Research, 2017, 137, 45-52.	0.8	54
17	[OP.3B.05] HEXARELIN PRESERVES MYOCARDIAL FUNCTION AND REDUCES INFLAMMATION AND FIBROSIS IN A MOUSE MODEL OF MYOCARDIAL ISCHEMIA REPERFUSION. Journal of Hypertension, 2017, 35, e29.	0.3	0
18	Radiological studies of fetal alcohol spectrum disorders in humans and animal models: An updated comprehensive review. Magnetic Resonance Imaging, 2017, 43, 10-26.	1.0	41

#	Article	IF	CITATIONS
19	A USPIO doped gel phantom for R2* relaxometry. Magnetic Resonance Materials in Physics, Biology, and Medicine, 2017, 30, 15-27.	1.1	4
20	T1 Mapping for Myocardial Fibrosis by Cardiac Magnetic Resonance Relaxometry—A Comprehensive Technical Review. Frontiers in Cardiovascular Medicine, 2017, 3, 49.	1.1	27
21	184â€Cardioprotective Role of Hexarelin in a Mouse Model of Myocardial Infarction. Heart, 2016, 102, A127.1-A127.	1.2	Ο
22	<scp>WorkWays</scp> : interacting with scientific workflows. Concurrency Computation Practice and Experience, 2015, 27, 4377-4397.	1.4	8
23	In vivo High Angular Resolution Diffusion-Weighted Imaging of Mouse Brain at 16.4 Tesla. PLoS ONE, 2015, 10, e0130133.	1.1	32
24	Carotid ultrasound pulsatility indices and cardiovascular risk in Australian women. Journal of Medical Imaging and Radiation Oncology, 2015, 59, 20-25.	0.9	9
25	Quantification of β-Amyloidosis and rCBF with Dedicated PET, 7 T MR Imaging, and High-Resolution Microscopic MR Imaging at 16.4 T in APP23 Mice. Journal of Nuclear Medicine, 2015, 56, 1593-1599.	2.8	10
26	The multi-modal Australian ScienceS Imaging and Visualization Environment (MASSIVE) high performance computing infrastructure: applications in neuroscience and neuroinformatics research. Frontiers in Neuroinformatics, 2014, 8, 30.	1.3	68
27	Differential Changes in Muscle Composition Exist in Traumatic and Nontraumatic Neck Pain. Spine, 2014, 39, 39-47.	1.0	87
28	Identification of Pre-Spike Network in Patients with Mesial Temporal Lobe Epilepsy. Frontiers in Neurology, 2014, 5, 222.	1.1	7
29	WorkWays: Interacting with Scientific Workflows. , 2014, , .		5
30	Current developments in MRI for assessing rodent models of multiple sclerosis. Future Neurology, 2014, 9, 487-511.	0.9	1
31	Visualization of mouse barrel cortex using ex-vivo track density imaging. NeuroImage, 2014, 87, 465-475.	2.1	21
32	Hippocampal volume and cell density changes in a mouse model of human genetic epilepsy. Neurology, 2013, 80, 1240-1246.	1.5	21
33	Non-Invasive Monitoring of Sucrose Mobilization from Culm Storage Parenchyma by Magnetic Resonance Spectroscopy. Bioscience, Biotechnology and Biochemistry, 2013, 77, 487-496.	0.6	5
34	Interpretation of Medical Imaging Data with a Mobile Application: A Mobile Digital Imaging Processing Environment. Frontiers in Neurology, 2013, 4, 85.	1.1	7
35	Ventilation distribution in rats: Part 2 – A comparison of electrical impedance tomography and hyperpolarised helium magnetic resonance imaging. BioMedical Engineering OnLine, 2012, 11, 68.	1.3	14
36	Super-resolution track-density imaging studies of mouse brain: Comparison to histology. NeuroImage, 2012, 59, 286-296.	2.1	105

3

#	Article	IF	CITATIONS
37	Segmentation of the C57BL/6J mouse cerebellum in magnetic resonance images. NeuroImage, 2012, 62, 1408-1414.	2.1	31
38	Association between congenital defects in papillary outgrowth and functional obstruction in <i>Crim1</i> mutant mice. Journal of Pathology, 2012, 227, 499-510.	2.1	10
39	Magnetic Resonance Imaging: The Underlying Principles. Journal of Orthopaedic and Sports Physical Therapy, 2011, 41, 806-819.	1.7	27
40	Segmentation of the mouse hippocampal formation in magnetic resonance images. NeuroImage, 2011, 58, 732-740.	2.1	88
41	MRI resolution enhancement: How useful are shifted images obtained by changing the demodulation frequency?. Magnetic Resonance in Medicine, 2011, 65, 664-672.	1.9	17
42	MRI demodulation frequency changes provide different information. Magnetic Resonance in Medicine, 2011, 66, 1513-1514.	1.9	2
43	The Temporal Development of Fatty Infiltrates in the Neck Muscles Following Whiplash Injury: An Association with Pain and Posttraumatic Stress. PLoS ONE, 2011, 6, e21194.	1.1	91
44	Magnetic resonance microscopy of the equine hoof wall: a study of resolution and potential. Equine Veterinary Journal, 2010, 38, 461-466.	0.9	11
45	Magnetic resonance spectroscopy: is it ripe for clinical practice?. Lancet Neurology, The, 2010, 9, 351.	4.9	0
46	A wrapped edge transverse gradient coil design for increased gradient homogeneity. Concepts in Magnetic Resonance Part B, 2009, 35B, 139-152.	0.3	4
47	The clinical presentation of chronic whiplash and the relationship to findings of MRI fatty infiltrates in the cervical extensor musculature: a preliminary investigation. European Spine Journal, 2009, 18, 1371-1378.	1.0	46
48	Combined approach for non-invasive measurement of liver pathology by MR. Journal of Hepatology, 2009, 51, 1083-1084.	1.8	1
49	Magnetic resonance imaging and spectroscopy accurately estimate the severity of steatosis provided the stage of fibrosis is considered. Journal of Hepatology, 2009, 51, 389-397.	1.8	156
50	1009 QUANTITATION OF STEATOSIS BY MAGNETIC RESONANCE IMAGING (MRI) AND SPECTROSCOPY (MRS) IN LIVER DISEASE: EFFECT OF HEPATIC FIBROSIS. Journal of Hepatology, 2009, 50, S365-S366.	1.8	0
51	Magnetic resonance imaging and spectroscopy for monitoring liver steatosis. Journal of Magnetic Resonance Imaging, 2008, 28, 937-945.	1.9	174
52	Feasibility of functional magnetic resonance lung imaging in Australia with long distance transport of hyperpolarized helium from Germany. Respirology, 2008, 13, 599-602.	1.3	14
53	An Approach of Deriving Relative Sensitivity Profiles for Image Reconstruction in MRI. IEEE Journal on Selected Topics in Signal Processing, 2008, 2, 817-827.	7.3	1
54	MRI study of the cross-sectional area for the cervical extensor musculature in patients with persistent whiplash associated disorders (WAD). Manual Therapy, 2008, 13, 258-265.	1.6	93

#	Article	IF	CITATIONS
55	Fatty infiltrate in the cervical extensor muscles is not a feature of chronic, insidious-onset neck pain. Clinical Radiology, 2008, 63, 681-687.	0.5	113
56	Validation of Mualem's Conductivity Model and Prediction of Saturated Permeability from Sorptivity. ACI Materials Journal, 2008, 105, .	0.3	4
57	Fatty Infiltration in the Cervical Extensor Muscles in Persistent Whiplash-Associated Disorders. Spine, 2006, 31, E847-E855.	1.0	230
58	A wave equation technique for designing compact gradient coils. Concepts in Magnetic Resonance Part B, 2006, 29B, 62-74.	0.3	3
59	The design of planar gradient coils. Part I: A winding path correction method. Concepts in Magnetic Resonance Part B, 2005, 27B, 17-24.	0.3	16
60	The design of planar gradient coils. Part II: A weighted superposition method. Concepts in Magnetic Resonance Part B, 2005, 27B, 25-33.	0.3	8
61	Magnetic resonance imaging analysis of the upper cervical spine extensor musculature in an asymptomatic cohort: an index of fat within muscle. Clinical Radiology, 2005, 60, 355-363.	0.5	50
62	The Use of Unwrapped Phase in MR Image SegmentationÂ: AÂPreliminaryÂStudy. Lecture Notes in Computer Science, 2005, , 813-820.	1.0	4
63	Use of spherical harmonic deconvolution methods to compensate for nonlinear gradient effects on MRI images. Magnetic Resonance in Medicine, 2004, 52, 115-122.	1.9	135
64	PROCESSING OF URINARY PHEROMONES IN ANTECHINUS STUARTII (MARSUPIALIA: DASYURIDAE): FUNCTIONAL MAGNETIC RESONANCE IMAGING OF THE BRAIN. Journal of Mammalogy, 2002, 83, 71-80.	0.6	4
65	Repeated Three-Dimensional Magnetic Resonance Imaging of Atherosclerosis Development in Innominate Arteries of Low-Density Lipoprotein Receptor-Knockout Mice. Circulation, 2002, 106, 1716-1721.	1.6	61
66	Magnetization transfer imaging for polymer gel dosimetry. Physics in Medicine and Biology, 2002, 47, 1881-1890.	1.6	59
67	MR image-based measurement of rates of change in volumes of brain structures. Part II: application to a study of Alzheimer's disease and normal aging. Magnetic Resonance Imaging, 2002, 20, 41-48.	1.0	53
68	Effect of Rosiglitazone on Insulin Sensitivity and Body Composition in Type 2 Diabetic Patients. Obesity, 2002, 10, 1008-1015.	4.0	191
69	4D deformation modeling of cortical disease progression in Alzheimer's dementia. Magnetic Resonance in Medicine, 2001, 46, 661-666.	1.9	107
70	Detection of dimethyl sulfone in the human brain by in vivo proton magnetic resonance spectroscopy. Magnetic Resonance Imaging, 2000, 18, 95-98.	1.0	27
71	A 1H MRS study of probable Alzheimer's disease and normal aging: implications for longitudinal monitoring of dementia progression. Magnetic Resonance Imaging, 1999, 17, 291-299.	1.0	121
72	Changes in the hippocampus induced by glucose in thiamin deficient rats detected by MRI. Brain Research, 1998, 791, 347-351.	1.1	23

5

#	Article	IF	CITATIONS
73	A reproducible method for automated extraction of brain volumes from 3D human head mr images. Journal of Magnetic Resonance Imaging, 1998, 8, 480-486.	1.9	13
74	Localized two-dimensional shift correlated spectroscopy in humans at 2 Tesla. Magnetic Resonance in Medicine, 1994, 32, 251-257.	1.9	38
75	Measurement of the T2 relaxation time of ethanol and cerebral metabolites,in vivo. Magnetic Resonance in Medicine, 1992, 23, 333-345.	1.9	25
76	The visibility of the1H NMR signal of ethanol in the dog brain. Magnetic Resonance in Medicine, 1991, 19, 340-348.	1.9	28
77	On the use of a slice-selective 270° self-refocusing Gaussian pulse for magnetic resonance imaging. Magnetic Resonance in Medicine, 1991, 19, 456-460.	1.9	2
78	High-field localized invivo proton spectroscopy on micro volumes. Magnetic Resonance in Medicine, 1990, 13, 518-523.	1.9	11
79	In vivo volumeâ€selective metabolite editing via correlated z â€order. Magnetic Resonance in Medicine, 1990, 16, 460-469.	1.9	9
80	Study of human liver disease with P-31 magnetic resonance spectroscopy Gut, 1990, 31, 463-467.	6.1	58
81	Metabolite editing via correlated z order with total inherent coherence. ECZOTIC. Journal of Magnetic Resonance, 1989, 83, 190-196.	0.5	4
82	The unequivocal determination of lactic acid using a one- dimensional zero-quantum coherence-transfer technique. Magnetic Resonance in Medicine, 1989, 9, 132-138.	1.9	26
83	In vivo high-resolution volume-selected proton spectroscopy andT1 measurements in the dog brain. Magnetic Resonance in Medicine, 1989, 9, 288-295.	1.9	10
84	Gradient-induced water-suppression techniques for high-resolution NMR spectroscopy. Journal of Magnetic Resonance, 1989, 81, 411-417.	0.5	5
85	Homonuclear coherence transfer experiments using shaped RF pulses having a tailored phase profile. Journal of Magnetic Resonance, 1989, 82, 597-604.	0.5	3
86	Nodal inhomogeneity mapping by localized excitation—the "NIMBLE―shimming technique for high-resolutionin Vivo NMR spectroscopy. Magnetic Resonance in Medicine, 1988, 7, 352-357.	1.9	12
87	The study of human organs by phosphorus-31 topical magnetic resonance spectroscopy. British Journal of Radiology, 1987, 60, 367-373.	1.0	38
88	A comparison of some gradient-encoded volume-selection techniques forin vivo NMR spectroscopy. Magnetic Resonance in Medicine, 1987, 4, 393-398.	1.9	25
89	On the calculation of magnetization slice profiles for NMR imaging andin vivo spectroscopy. Magnetic Resonance in Medicine, 1987, 5, 478-484.	1.9	2
90	Water-suppressed volume-selected1H NMR spectroscopy in viva: Application to study tumor metabolism. Magnetic Resonance in Medicine, 1987, 5, 508-512.	1.9	8

#	Article	IF	CITATIONS
91	A simple modification for the elimination of phase distortions, a characteristic of "binomial―solvent suppression pulse sequences. Journal of Magnetic Resonance, 1987, 74, 184-187.	0.5	8
92	Improvements and extensions to the DIGGER technique for performing spatial selective excitation. Journal of Magnetic Resonance, 1987, 73, 360-368.	0.5	9
93	Application of surface coil reception to record volume-selected high-resolution proton in vivo spectra using a combined DIGGER-SPACE pulse sequence. Journal of Magnetic Resonance, 1987, 73, 159-167.	0.5	8
94	Assessment of human liver metabolism by phosphorus-31 magnetic resonance spectroscopy. British Journal of Radiology, 1986, 59, 695-699.	1.0	103
95	Are quenches dangerous?. Magnetic Resonance in Medicine, 1986, 3, 112-117.	1.9	7
96	The utilization of two frequency-shifted sinc pulses for performing volume-selectedin vivoNMR spectroscopy. Magnetic Resonance in Medicine, 1986, 3, 970-975.	1.9	17
97	Discrete isolation from gradient-governed elimination of resonances. DIGGER, a new technique for in vivo volume-selected NMR spectroscopy. Journal of Magnetic Resonance, 1986, 70, 319-326.	0.5	45
98	Water signal elimination in Vivo, using "suppression by mistimed echo and repetitive gradient episodes― Journal of Magnetic Resonance, 1986, 70, 176-180.	0.5	31
99	First year of experience with P-31 magnetic resonance studies of human liver. Magnetic Resonance Imaging, 1986, 4, 413-416.	1.0	19
100	SUXAMETHONIUM CHLORIDE AND MALIGNANT HYPERPYREXIA. British Journal of Anaesthesia, 1986, 58, 447-450.	1.5	32
101	A mitochondrial encephalomyopathy. Journal of the Neurological Sciences, 1985, 71, 105-118.	0.3	65
102	PHOSPHORUS-31 NUCLEAR MAGNETIC RESONANCE STUDIES OF MUSCLE METABOLISM IN MALIGNANT HYPERPYREXIA. British Journal of Anaesthesia, 1984, 56, 663-664.	1.5	7
103	THE EFFECT OF THE CALCIUM ION ANTAGONIST 8-(N,N-DIETHYLAMINO)-OCTYL-3,4,5-TRIMETHOXYBENZOATEON MALIGNANT HYPERPYREXIA-SUSCEPTIBLE PORCINE SKELETAL MUSCLE. Clinical and Experimental Pharmacology and Physiology, 1983, 10, 587-593.	0.9	3
104	CLODANOLENE SODIUM AND MALIGNANT HYPERPYREXIA. British Journal of Anaesthesia, 1982, 54, 1237.	1.5	1
105	Regional rates of brain atrophy - can they be used as a reliable tool for early diagnosis of Alzheimer's disease?. , 0, , .		2
106	Cardiac Magnetic Resonance T1 Mapping in Cardiomyopathies. , 0, , .		0
107	TissueStack: a new way to view your imaging data. Frontiers in Neuroinformatics, 0, 7, .	1.3	0
108	TissueStack: an Open Source HTML5 web based imaging viewer. Frontiers in Neuroinformatics, 0, 7, .	1.3	0

#	Article	IF	CITATIONS
109	A segmentation guide and probabilistic atlas of the C57BL/6J mouse brain from magnetic resonance imaging. Frontiers in Neuroinformatics, 0, 8, .	1.3	0